Egypt. J. Chem. **Vol. 67**, No. 8 pp. 569 - 583 (2024)

Egyptian Journal of Chemistry

http://ejchem.journals.ekb.eg/

Synthesis and Investigation of New Pyridine Metal Complexes as Possible Antibacterial Agents Against Digestive System Harmful Bacteria Causing Human Malnutrition

Maged S. Al-Fakeh [a,b], Aiyeshah Alhodaib [c], Wael A. El-Sayed [a]

[a] *Department of Chemistry, College of Science, Qassim University, Buraidah 51452, Saudi Arabia.*

[b] *Taiz University, Taiz 3086, Yemen.*

[c] *Department of Physics, College of Science, Qassim University, Buraydah 51452, Saudi Arabia.*

Abstract

Bacterial resistance to the current applied antibacterial drugs represents an important threat to human health and overcoming such an issue is a critical challenge. Metal-based medications constitute a useful chemotherapeutic approach possessing the possible ability to overcome drug resistance because of their unique structural characteristics and related distinct modes of action. In the current study, the pyridyl-arylidine shiff base ligand (formed from 2-amino-3-methylpyridine and salicylaldehyde) interacted with a number of transition metals (Pd(II), Co(II), Cu(II), and Ag(I)) resulting in the formation of the corresponding metal complexes. Thermal analysis, the appropriate spectroscopic tools (1H-NMR, FT-IR, and UV-vis.), molar conductivity, magnetic moment, and elemental analyses were applied to investigate the afforded HL and the derived compounds. Thermal analysis besides C.H.N analytic results verified the formulae of the Schiff base ligand and metal compounds. The compounds (Pd(II), Co(II), Cu(II) and Ag(I) revealed electrolytic behavior as shown by their molar conductivity values. The obtained Pd(II) and Cu(II) complexes exhibited square planar geometrical shapes, except for the Co(II) and Ag(I) complexes, which displayed tetrahedral geometry. Thermal analysis results revealed that the Pd(II), Co(II) and Cu(II) complexes consistently liberate ligands and anionic components following; the initial loss of H2O molecules of hydration. Besides the purity confirmation of the investigated samples, XRD diffraction patterns elucidated their lattice dynamics. They demonstrated that the complexes of Co(II) and Ag(I) have a crystalline structure revealing a particular average size, of the crystallites. The resulting metal complexes were investigated for their antimicrobial activity and demonstrated superior antibacterial efficiency than the free un-complexed legend. Interestingly, cobalt and silver-based complexes showed potent activity against E. coli that were found to be more potent than those recorded for Neomycin. Molecular docking results for defining and anticipating the inhibitory potential and binding procedure of generated ligand with 3ty7, 3t88 and 5k04 receptors for Staphylococcus Aureus, Escherichia coli and Candida albicans, respectively were investigated.

Keywords: Pyridine - Schiff's base - ligand, complexes, spectral studies, antibacterial - antimicrobial activity, molecular docking.

1. Introduction

Antimicrobial resistance to a variety of antibiotics has been dramatically enlarged worldwide representing a considerable threat to human health and multidrug-bacteria resistance (MDR) has continually posed intensive global health challenges for drug development research [1-13]. Besides lack of food supply, starvation, or other economic and social reasons, it has been found that malnutrition may also exist due to health problems that impede the absorption of food in the digestive system and may

*Corresponding author e-mail: Email: m.alfakeh@qu.edu.sa.(Maged S. Al-Fakeh)
Received date 12 May 2024; revised date 29 May 2024; accepted date 12 June 2024
DOI: 10.21608/EJCHEM.2024.289004.9700

even lead to health damage and diseases. Although, types of bacterial strains live inside the colon permanently, and most of them coexist with humans without harm behavior, some of them may result in infection with some diseases such as food poisoning that may cause death in addition to several bacterial diseases. Accordingly, it's now impossible to neglect or avoid developing strategies, for the iteration of treatment potencies against their infections. On the way for the creation and development of medications with distinct modes of action, a considerable denomination of chemotherapeutic medicines with a possible potential to overcome drug resistance is metal-based medications. Compounds incorporating metals via a coordinating linkage may achieve successful access to possible unique modes of action due to their possible existence widely as three-dimensional geometries rather than un-complexed organic products [14]. The latter significance allowed them promising precursors for the generating new antibacterial drugs to struggle the increased threat of emerging resistance. The investigation of large number of metal-incorporating products revealed by the (CO-ADD) Community for Open Antimicrobial Drug Discovery have been recorded for antimicrobial activity. Metal-incorporating derivatives revealed significantly higher hit-rate reaching about 9.9% in comparison with the single organic molecules which showed 0.87% in the CO-ADD database and eighty-eight provided activities for at least one of the strains [15]. Metal compounds have played a decisive role in medicinal applications [16,17] and have been outstanding as a useful cornerstone of medicinal chemistry since Cisplatin (chemotherapeutic platinum-based drug) was approved [18]. The complexation of transition metals has opened many doors for scientists and further broadened their areas of expertise in chemistry, biology, materials sciences, and industries. Here are some key reasons for their importance: Here are some key reasons for their importance: Biological activity: Most of the metallic complexes i. e. , are involved in many physiological activities inside the body. As for metal ions, such as cobalt(II), copper(II), palladium(II), and silver(I), they form the central part of some crucial enzymes and proteins related to metabolism, DNA replication, and signaling pathways. The metals as drug molecules, e.g. cisplatin in chemotherapy of cancer, are used to condition the chemical reactivity of metal complexes in order to take advantage of certain biological processes. Additionally, catalysis, materials science, electronics, Optoelectronics, environmental applications, medicine and imaging [19-21]. Recently, numerous Ti, Fe, Ru, Pd, Au, Ag, and Cu-incorporating metal compounds have reached human clinical trials for treatments for malaria, cancer, and neurodegenerative diseases [22-24]. A palladium-based photo-dynamic therapy agent, was confirmed for treatment of prostate cancer [25]. Additionally, metal coordination complexes possess access to unparalleled styles of action: ligand exchange or release, catalytic generation, redox activation, and ROS generation of toxic species. The latter characteristic mechanisms are not impossible to replicate by non-complexed organic complexes [26,27]. One of the structural characteristics of metal complexes is the ability to achieve superior targeted three-dimensional geometry [28]. Figure 1 shows one of the investigated Pd complexes with antibacterial activity [29]

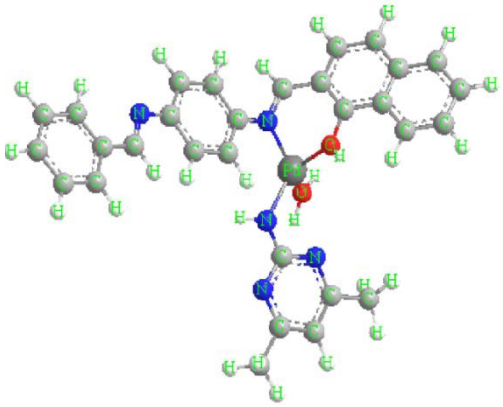

Fig. 1: Antibacterial pyridine core ligand-based Pd(II) complex

Schiff bases represent a group of interesting functionalized ligands providing a variety of complexes due to their excellent chelating behavior, and acquired greater attention because of their structural flexibility, and the unique characteristics of the C=N linkage [30-35].

The C=N in Schiff's base connection plays a significant role in the demonstration of biological activity, due to the discovery that the lone pair of electrons of the nitrogen atom of the hybridized orbital has chemical and biological significance [36-38]. In the chemistry of metals, coordination Schiff bases are considered "privileged ligands", which means that they are employed in a variety of industries and fields, including chemistry, organic synthesis, and optical and electrochemical sensors. In addition, transition metal complexes of Schiff bases also represent a wide range of medicinal chemistry applications [39-40]. On the other hand, pyridine derivatives have been extensively found as promising compounds achieving a broad spectrum of bioactivities among which antimicrobial and anticancer activities were, interestingly, revealed [37-39]. Figure 2 presents biologically active complexes

incorporating a substituted pyridine ligand [35,41]. The afforded results revealed improved antibacterial results of the same metals with other ligands such as alginate/carrageenan crosslinked biopolymer and study of the antibacterial, antioxidant, and anticancer performance of its Mn (II), Fe (III), Ni (II), and Cu (II) polymeric complexes. Our new prepared compounds showed higher activity on microbes than previous metals and ligands [30]. The pyridine core system in addition to other metal complexes were characterized with their potent antimicrobial activity [42-43]. The above significances and our interest in the synthesis of new structures as possible potent antimicrobial candidates promoted our interest in the current investigation for the preparation of pyridine-arylidene hybrids and studying their antimicrobial activities. The formation of the later molecular hybridized complexes was hypothesized to afford more biologically active candidates. The achievements of producing possible potent antibacterial agents which will fight digestion system microbe and acquiring full food interest will help overcome the generated malnutrition by the attack of such microbes.

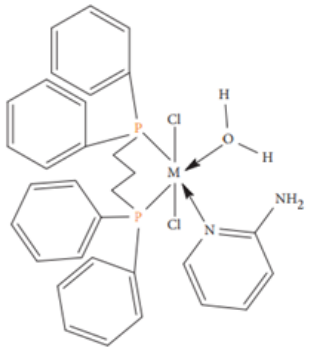

Fig. 2: Pyridine based complexes, M = Mn(II), Ni(II), Cu(II), or Fe(II).

2. Materials and reagents:

All chemicals, reagents, and media utilized in the current investigations were of analytical quality and analytical grades (Sigma-Aldrich and Across). The used chemicals can be found in in details in the experimental procedures for the preparation of ligands and complexes.

2.1. Instruments

The supplemental information provided a full description of the instruments utilized for measuring microanalyses (C, H, and N), IR, molar conductivity, mass, electronic spectra, ^{1}H-NMR spectra, thermo-gravimetric (TG and DTG), and as well as XRD. The additional information provided details on the techniques used to assess the antibacterial and anti-cancer properties.

2.2. Preparation of the ligand

HL ligand: 2-(((3-Methylpyridin-2-yl)imino)-methyl)phenol

To a stirred solution of 2-amino-3-methylpyridine (10 mmol) in absolute ethanol (30 mL) was added 5 drops of glacial acetic acid. 2-Hydroxybenzaldehyde (10 mmol) was added dropwise to the reaction of the mixture while stirring then the resulting mixture was heated under reflux while stirring for 7 h after which TLC indicated completion of the reaction (pet. ether - ethyl acetate; 3:1). The solvent was reduced, under vacuum, to half of its original amount and the remaining was cooled to room temperature then allowed to stand for 3 hours at r.t., The resulting precipitate was filtered, then washed with cold ethanol, dried and recrystallized by ethanol, to give the ligand as a yellowish powder [42]. Yield: 79%, m.p. is 192-193 °C. Anal. Calcd. for $C_{13}H_{12}N_2O$: Carbon, 73.56; Hydrogen, 5.70; Nitrogen,13.20%; Found: Carbon, 73.14; Hydrogen, 5.64; Nitrogen, 12.83% [44].

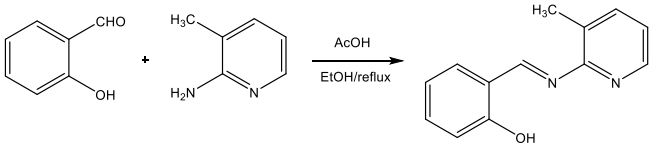

Scheme 1: Preparation of the pyridyl arylidine ligand

2.3. Preparation of the transition and non-transition metal complexes

[ML] To the 2-(((3-Methylpyridin-2-yl)imino)methyl)phenol ligand (MPIMP) ligand, 1.6 mmol (0.6 g) stirred in 20 mL of ethanol, was added in small portions of $PdCl_2$ (1.3 mmol, 0.50 g), $CoCl_2$.$6H_2O$ (1.6 mmol, 0.56 g), $CuCl_2$.$2H_2O$ (1.2 mmol, 0.40 g) or $AgNO_3$ (1.2 mmol, 0.47 g). The color of the reaction mixture complexes changed after a few minutes and was refluxed for 3 h. The precipitated solid prepared on cooling was filtered, then washed with EtOH, and dried. The same procedure was used to synthesize and isolate the ML1 compounds.

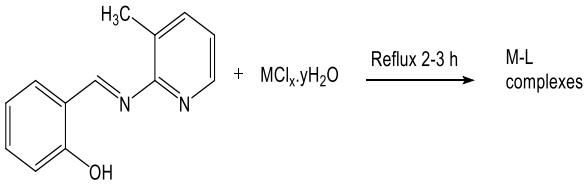

Scheme 2: Preparation of the metal complexes.

2.4. Antimicrobial activity

2.4.1. Antibacterial investigation

The anti-microbial activity of the prepared metal compounds was studied by the cup diffusion agar method [45,46].

2.4.2. Minimum bactericidal concentrations (MBC's) of each compound

The MBC method was conducted in a procedure that is fulfilled with that previously reported [45].

2.4.3 Molecular docking

Auto Dock 4.2 was applied for investigating the docking of the functionalized centers and the details as well as parameters were provided in the supplementary file.

3. Results and discussion:

The legend incorporating the pyridine system and aryl part linked via an arylidene linkage as a Schiff base type was prepared by the reaction of 2-amino-3-methylpyridine with 2-hydroxybenzaldehyde in ethanol as a solvent. The metal compounds were synthesized by the reaction of 2-(((3-methylpyridin-2-yl)imino)methyl)phenol ligand (MPIMP) and metal chlorides or nitrate. These components were found to react in the molar ratio 1: 1: Metal: MPIMP. The complexes are air-stable, and soluble in common organic solvents. The molar conductivity values ΛM of the ligand and complexes in 10^{-3} M dimetylsulphoxide solutions vary from 10.5 for the ligand to 12.55, 24.9, 25.3, and 15.2 S cm^2 mol^{-1} for the Pd(II), Co(II), Cu(II) and Ag(I) complexes respectively, thus revealing their non-electrolytic character. The compositions of the ligands and compounds are supported by the analytical and physical data recorded in Table (1).

Table 1: Physical data and analytical for the ligand and metal complexes.

Compounds	M.F M.W	Color Yield (%)	Found (Calcd. %) C	 H	 N	m.p.°C (Decom.)
Ligand (MPIMP)	$C_{13}H_{12}N_2O$ 212.25	Yellow	73.80 73.55	5.93 5.69	13.42 13.19	**110**
[Pd(MPIMP)Cl(H_2O)]	$C_{13}H_{13}N_2PdO_2Cl$ 371.14	Reddish-Brown 74.5	42.48 42.06	3.98 3.52	7.92 7.54	**165**
[Co(MPIMP)Cl(H_2O)].H_2O	$C_{13}H_{15}N_2CoO_3Cl$ 341.59	Light-Brown 80.9	46.03 45.70	4.96 4.42	8.75 8.19	**150**
[Cu(MPIMP)Cl(H_2O)].H_2O	$C_{13}H_{15}N_2CuO_3Cl$ 346.2	Light-Green 76.5	46.14 45.09	4.88 4.36	8.84 8.09	**128**
[Ag(MPIMP)NO_3]	$C_{13}H_{11}N_3AgO_4$ 381.07	Creamy-White 78.1	41.16 40.97	3.01 2.90	10.96 11.02	**142**

3.1. FT-IR Spectroscopy

The principal "infrared spectra" of the legend demonstrated the absence of bands at 1607, 1556, and 1110 cm^{-1} due to ν(HC=N), (=N), and ν(C-N) in ring stretching vibrations. The IR spectrum of the fabricated Pd(II), Co(II), Cu(II), and Ag(I) compounds are illustrated in Table (2). When the FT-IR spectra of compounds 1-4 were compared to those of the free (MPIMP) ligand, interesting features relating to "metal-ligand (M-L) interactions" were observed. The band at 1607 recorded to pyridine ring ν(C=N) nitrogen also, shifted to a lower or higher frequency by 5-13 cm^{-1} which was indicative of involvement, of ring-N, of pyridine in chelation [47]. Briefly, through oxygen and nitrogen atoms, the MPIMP ligand coordinates to metal ions in bidentate mode except for Ag(I) in tridentate mode. A broad, moderately intense band in the range 3309-3181 cm^{-1} was appointed to ν(OH) of (H_2O) for Pd(II), Co(II), and Cu(II) complexes [48,49]. In addition, the demonstration of absorption bands, which are representative characteristic absorption peaks at 550-542 cm^{-1} and 464-445 cm^{-1} correspond to" ν(metal-oxygen) and ν(metal-nitrogen), respectively [50]. The FT-IR spectra of the Pd(II), Co(II), and Cu(II) complexes appear as a band at 430-412 cm^{-1} recorded

to (M-Chlorine) [51]. The Ag(I) complex showed a strong band attributed to the characteristic ν (N-O) vibration of the (NO_3^-) at 1369 cm^{-1} and the medium band at 813 cm^{-1} [52].

Table 2. Characteristic IR-spectra data (cm^{-1}) of the complexes studied.

Assignment	MPIMP Ligand	Pd(II) complex	Co(II) complex	Cu(II) complex	Ag(I) complex
υ(O-H) lattice water		-	3309	3321	-
υ(O-H) coordinated water	-	3187	3181	3183	-
s, HC=N	1607	1604	1611	1602	1620
s, =N	1556	1591	1561	1564	1584
υC-$N_{in\ ring}$	1110	1082	1050	1040	1041
M-O	-	542	547	545	550
M-N	-	464	445	458	453
M-Cl	-	430	415	412	-

3.2. NMR spectra

The Spectral assignments changes in the revealed chemical shifts was resulted owing to the coordination process between the ligand and ion in the formed complexes. The H NMR spectra of the aryl-pyridyl Shiff bas ligand revealed the chemical shifts 2.37 (s, 3H, CH_3), 6.97-7.00 (m, 2H, Ar-H), 7.40-7.42 (m, 1H, Ar-H), 7.47-49 (m, 1H, Ar-H), 7.77-7.79 (m, 2H, Ar-H), 8.39 (d, 1H, *J* = 8.4 Hz, Ar-H), 9.49 (s, 1H, CH=N), 13.05 (s, 1H, OH). The complexation process resulted in various clear shifts in the assignments.

Thus, the chemical shift of the methyl and the methine hydrogen (C*H*=N) of the pyridyl Schiff base ligand, which was initially seen at 2.37 and 9.45 ppm, respectively has been slightly altered to 2.42 and 9.62 ppm, respectively in the formed Pa complex as a representative example. The fully conjugated feature in the aromatic system of the complex that was affected by the coordination reaction also influences the chemical shifts of the aryl protons in the formed complex. Accordingly, the signals of the aryl and pyridyl protons also revealed variation and a degree of certain shifts and was revealed at 6.70-8.60 ppm. The latter consequence is obviously due to the formation of the complex, and its displacement can be attributed to the alteration in the carbon framework of the Schiff base ligand due to its interaction with metal ions.

3.3. Electronic spectra, and magnetic susceptibility

The electronic spectra of the ligand 2-(((3-Methylpyridin-2-yl)imino)methyl)phenol (MPIMP) and its Pd(II), Co(II), Cu(II), and Ag(I) compounds in DMSO present two absorption maxima located in the regions 34,482 and 27,932 cm^{-1} assigned to π $\longrightarrow$ π* and n $\longrightarrow$ π* transitions within the organic ligand. The electronic spectral data and effective magnetic moment values; (B.M.) are shown in Table (3).

3.3.1. Palladium(II) compound

The electronic spectra of the palladium(II) compound have been listed in DMSO in region 200-700 nm, and the Pd(II) complex displays a band at 415 nm which is recorded to $^1A_{1g} \rightarrow {}^1E_g$ transition, indicating; square planar geometry around the palladium(II) ion [53]. The Pd(II) complex was 0.64 B.M., confirming the metal center's square planar geometry [54].

3.3.2. Cobalt(II) compound

The electronic absorption spectrum of the Co(II) compound exhibits only one band in the visible region at; 635 assigned to the $^4A_2$ (F) $\rightarrow {}^4T_1$ (F) transition, which indicates a tetrahedral structure [55]. The magnetic susceptibility value is found to be 4.20 B.M for the Co(II) compound which is indicative of tetrahedral structure [56].

3.3.3. Copper(II) compound

The Electronic Spectra of the Cu(II) compound demonstrate this characteristic band, at 472 nm which suggests, the square planar structure around the Cu(II) Centre. It shows this characteristic band at 472 nm due to $^2B_{1g} \rightarrow {}^2A_{1g}$ transition [57]. It's well known that for square-planar Cu(II) compounds, the magnetic moment value falls, in 1.82-1.86 B.M. A value of 1.84 B.M. for Cu(II) ion has been shown which is well within the expected region, found for square-planar Cu(II) complex [58].

3.3.4. Ag(I) compound

According to the electronic spectrum of the Ag(I) compound, the wavelengths were in 30, 120 -34, 246 cm^{-1} which may be assigned to n → π*, and π → π* transitions and an Ag→L charge transfer (CT), in which the ligand manifold includes π-system of the ligand suggesting tetrahedral geometry [34].

The suggested structures for the complexes are shown (Fig. 3) as follows:

Table 3: Eelectronic spectra to the ligand and their compounds.

Compounds	λ max (nm)	νmax (cm^{-1})	Assignment	Meff B.M
Ligand (MPIMP)	358 290	27,932 34,482	n → π* π → π*	- -
Pd(II) complex	415 372 295	24,096 26,881 33,898	$^1A_{1g} \rightarrow {}^1E_g$ n → π* π → π*	0.64
Co(II) complex	635 342 298	15,748 29,239 33,557	$^4A_2(F) \rightarrow {}^4T_1(F)$ n → π* π → π*	4.20
Cu(II) complex	472 348 302	21,186 28,735 33,112	$^2B_{1g} \rightarrow {}^2A_{1g}$ n → π* π → π*	1.84
Ag(I) complex	332 292	30,120 34,246	n → π* π → π*	diamagnetic

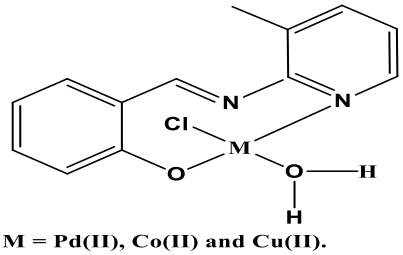

M = Pd(II), Co(II) and Cu(II).

Fig. 3. a): Suggested structures of [M(MPIMP)Cl(H_2O)].xH_2O where M = Pd(II), Co(II), Cu(II), x =1

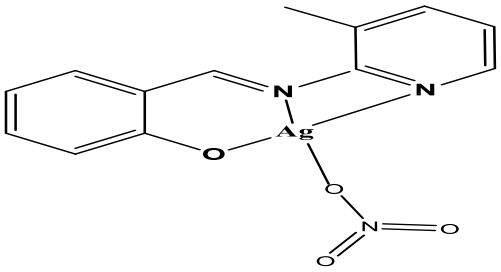

Fig. 3. b): Suggested structure of [Ag(MPIMP)NO_3]

3.4. Thermal Studies

Ag(I) complex

The thermogram of the silver(I) complex shows three steps of decomposition, with temperatures ranging from 60-148, 150-342, and 344-750 °C. The noticed mass loss of the first stage (60-148 °C), in the T.G curve agrees, with the loss of nitrate ion (calc. 16.27%, found at 15.98%) (DTG peak at 150 °C). This stage is marked on the DTA curve with a broad exothermic peak at 152 °C. The second and third steps lead to the decomposition of the remaining ligand(calc. 55.69 %, found. at 52.30 %). Thermogravimetry peaks at 250, and 490 °C, and the differential thermal analysis trace shows two endothermic peaks at 252 and 492 °C. The residual may be a silver oxide (calc. 32.50 %, found. at 31.72 %). The results revealed a good agreement between the calculated results and the suggested formulae, for weight loss of the complexes (Table 4 and Figure 4).

Table 4: Thermal analysis of the Pd(II), Co(II), Cu(II), and Ag(I) compounds.

Complexes	Step	Temp. Rang °C	TGA (Wt. loss %) Found	Calc.	Assignment
Pd(II) complex	**1st**	64-160	4.85	4.29	Loss of H_2O molecule
	2nd	162-246	9.55	9.04	Loss of Cl atom
	3rd	248-350	57.18	54.98	Decomposition of the MPIMP with the formation of PdO
	4th	352-750	32.97)	31.69	
Co(II) complex	**1st**	66-180	10.55	10.08	Loss of $2H_2O$ molecules
	2nd	182-302	10.37	10.15	Loss of Cl atom
	3rd	304-450	62.13	61.92	Decomposition of the MPIMP with the formation of CoO
	4th	452-750	16.94	16.85	
Cu(II) complex	**1st**	64-152	10.41	10.33	Loss of $2H_2O$ molecules
	2nd	154-250	10.23	9.96	Loss of Cl atom
	3rd	252-402	61.30	57.74	Decomposition of the MPIMP with the formation of CuO
	4th	404-592	22.97	21.93	
	5th	594-750			
Ag(I) complex	**1st**	60-148	16.27	15.98	Loss of $3H_2O$ molecules
	2nd	150-342	55.69	52.30	Loss of Cl atom
	3rd	344-750	32.50	31.72	Decomposition of the MPIMP with the formation of AgO

3.5. X-Ray Powder Diffraction

The X-ray patterns of chemically synthesized complexes as shown in Figure (5) were obtained "between the 2θ region starting from 10° to 80°". Figures reveal crystallographic structures, whereas the atoms were arranged in the triclinic position except Pd(II) complex in the monoclinic position. Table (5). These XRD spectra of the Pd(II), Co(II), Cu(II) and Ag(I) complexes indicate the number of prominent diffraction peaks at particular angles. The crystallite size increases with increases in peak intensity, directly proportional and inversely proportional to the full width, at half maxima (FWHM). The protruding peaks were used to calculate; the grain size via the, (Scherrer equation) expressed as follows:

$$D = (K \lambda)/(\beta \cos\theta)$$

where "D is the average crystallite size in Å, λ reveal the wavelength of the X-ray source (1.540) used in

XRD, β denote FWHM (full width at half maximum of the diffraction peak), K is the Scherrer constant (ranges from 0.9 to 1) and θ is the Bragg angle".

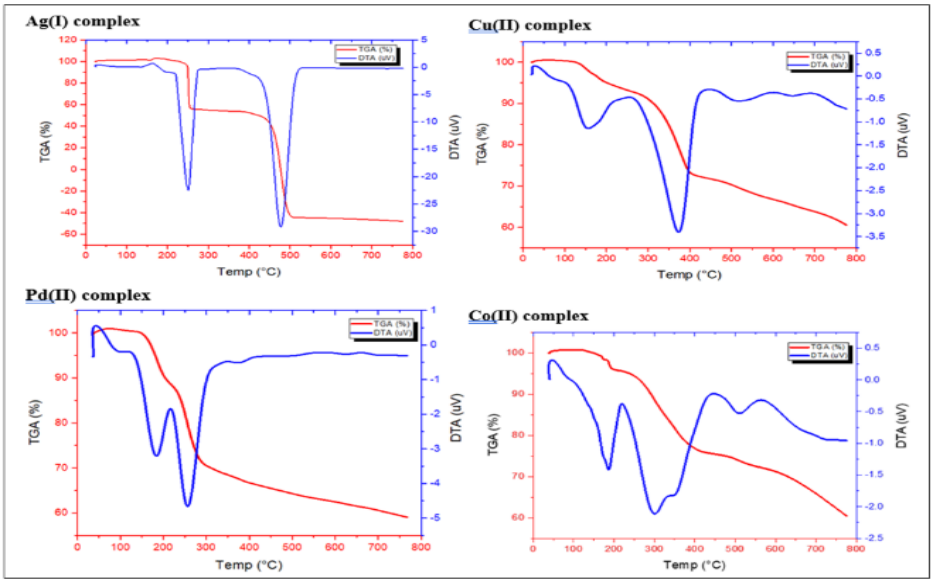

Fig. 4: Thermal analysis of the complexes

Table 5: X-Ray powder diffraction crystal data of the Pd(II), Co(II), Cu(II) and Ag(I) compounds.

Parameters	Pd(II) complex	Co(II) complex	Cu(II) complex	Ag(I) complex
Empirical formula	$C_{13}H_{13}N_2PdO_2Cl$	$C_{13}H_{15}N_2CoO_3Cl$	$C_{13}H_{15}N_2CuO_3Cl$	$C_{13}H_{11}N_3AgO_4$
Formula Weight	371.14	341.59	346.2	381.07
Crystal system	Monoclinic	Triclinic	Triclinic	Triclinic
a (Å)	9.520	6.593	3.429	1.888
b (Å)	6.195	12.746	5.651	7.982
c (Å)	11.197	15.352	14.853	9.757
Alfa (◦)	90.00	45.858	66.081	106.541
Beta (◦)	99.74	87.129	82.282	93.953
gamma (◦)	90.00	115.149	79.715	82.104
Volume of unit cell ($Å^3$)	650.90	709.28	258.24	139.57

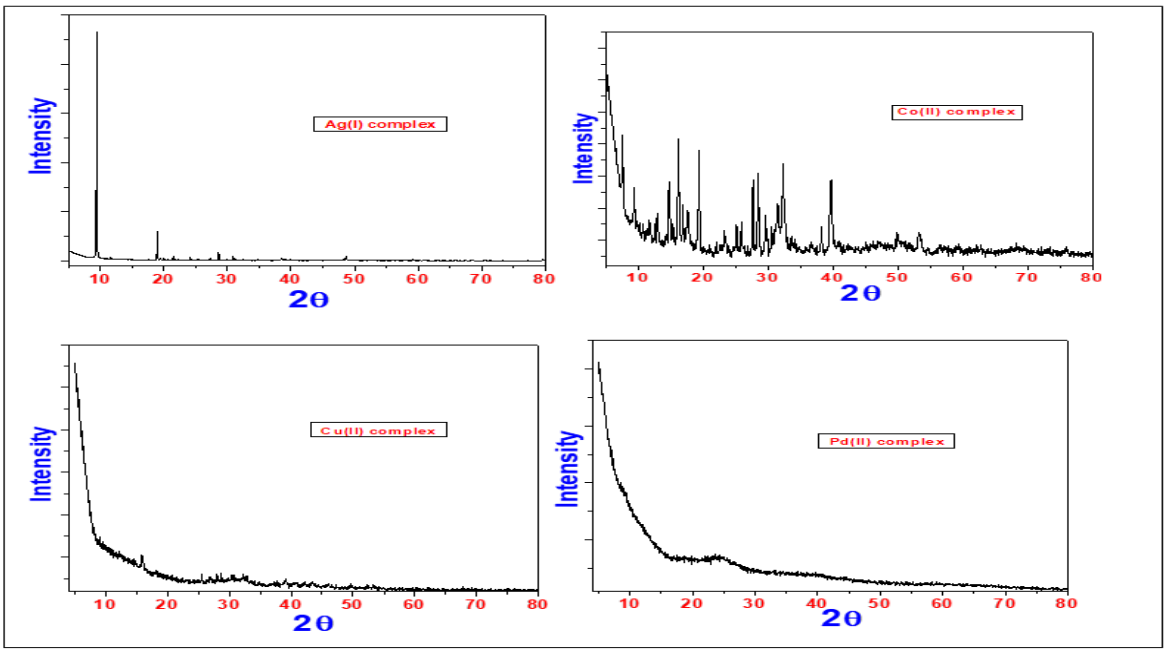

Fig. 5: XRD of the complexes.

3.6. Antimicrobial activity

The anti-microbial activity of the prepared metal compounds was tested by the cup diffusion agar method. The investigated representative test microbes that have been used were *Escherichia coli* ATCC 25933 (G-ve), *Staphylococcus aureus* ATCC 6538-P (G +ve), *Aspergillus niger* NRRL-A326 (fungus), and *Candida albicans* ATCC 10231 (yeast).

DD

Table 6: The antimicrobial activity of the metal complexes against different test.

Compound	Clear zone (mm)			
	S. aureus	*E. coli*	*C. albicans*	*A. niger*
Ligand	12	0	0	16
Co(II)	28	26	17	20
Pd(II)	25	24	22	19
Ag(I)	27	26	24	16
Cu(II)	13	14	16	23
Neomycin	31	25	29	0
Cyclohexamide	0	0	0	36

The metal complexes of cobalt(II), silver(I) followed by palladium(II) were the most potent among the series of the newly tested compounds and demonstrated distinctive activity against both *S. aureus* and *E. coli* organisms with inhibition zones relative to those recorded for the reference compounds. Interestingly, the activity of the metal complexes of cobalt(II) and silver(I) showed potent activity with large inhibition zones against *E. coli* that were found more potent than those recorded for reference drug Neomycin in the current investigation.

The inhibition zone diameters, of the tested complexes are shown in (Table 6). Generally, the results, revealed the observation that the most susceptible organisms were *S. aureus* and *E. Coli*, exhibiting relatively more sensitivity to three of the tested metal complexes. It was also obvious that the activity afforded for the metal complexes was higher than that recorded for the unbound ligand (Figure 6).

The silver metal complex was the most active compound against *C. albicans* followed by palladium showing moderate behavior. On the other hand, the results revealed that the ligand did not show any activity against *C. albicans* and *E. coli* while it possessed weak activities related to *S. aureus* and *A. niger*. Although, the lowest inhibition zones were shown for the *A. niger* fungal species, it showed to be moderately sensitive to the copper(II) complex (Table 5).

Structure-activity relationship: To attain the possible structure-activity relationship according to the results, the inactivation effects, and the afforded minimum inhibitory concentrations (MICs), values for the produced complexes were investigated for four studied microbial types. The resulted, data from the MIC data; revealed a variability in the inhibitory

concentrations of each complex against the targeted microbial strains (Table 7).

Table 7: MIC and MBC of the complexes against different test microbes

Sample	*Staphylococcus aureus*		*Escherichia coli*		*Candida albicans*	
	MIC µg/ml	**MBC µg/ml**	**MIC µg/ml**	**MBC µg/ml**	**MIC µg/ml**	**MBC µg/ml**
Co(II)	78.12	156.25	39.063	312.5	78.125	312.5
Pd(II)	9.77	39.063	19.53	78.125	312.5	625
Ag(I)	4.88	4.88	4.88	9.77	4.88	19.53

Trying to correlate the structural feature, represented by the nature and type of the metal in this investigation, it has been found that the arylidene substituted pyridine complexes incorporating Pd(II) and Ag(I) as coordinated metals showed improved activities ranged from high to potent activities against the bacterial species *S. aureus*, *E. coli* and *C. albicns*, revealing more potent activity higher than Cyclohexamide in case of silver(I) against *E. coli*. In addition, the pyridyl-arylidine complex possessing Cu^{++} metal revealed an observed selectivity against *A. niger* species. The results also indicated the potential effect of coordination of the studied metals with the legend which is clear by the preparation of metal complexes with distinctly improved activities relative to or higher than the reference compounds.

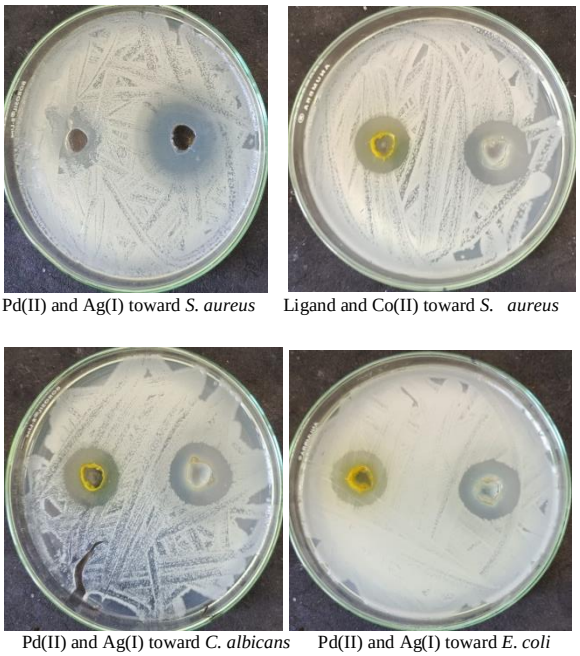

Pd(II) and Ag(I) toward *S. aureus* Ligand and Co(II) toward *S. aureus*

Pd(II) and Ag(I) toward *C. albicans* Pd(II) and Ag(I) toward *E. coli*

Fig. 6: Microbiological screenning of prepared compounds toward bacteria and fungi.

Prebiotic activity: The purpose of prebiotic activity investigation is the enhancement of growing gut microflora. Consequently, the activities of the Co(II), Ag(II) and Pd(II) complexes were studied. The basis for such investigation mainly depends on the comparison of the growths densities of the beneficial bacteria *Lactobacillus reuteri*, and *Lactobacillus casei* (probiotics) with those related to the pathogenic. All studied complexes revealed certain degree of prebiotic activity with *L casei* and *L. Reuteri* since the lowest prebiotic index (I) was recorded in case of Co(II)-Complex with *L.reuteri* (I = 1.5) while the most higher prebiotic index was observed for against *L.casei* (I = 3.9).

3.7. Molecular docking study

The behavior of the active compounds towards proteins was studied by Auto Dock since demonstration of the possible interaction patterns is one of the most important biological benefits of such products as possible ligands. Docking of Co complex into the active site of 3ty7 protein for investigating its possible interactions and binding patterns with the protein amino acids was performed.

Figures (7-12) show that the estimated legend Co(II) complex can achieve a good interaction with all receptors and produce results that are comparable. The studied protein has easily observable inter-hydrogen bonds since for visualizing the afforded interactions two- and three-dimensional images were used. The latter graphics may strongly contribute to the demonstration of the mechanism of interaction within docking molecules (Figures 6-11). The interaction between the studied complexes and the amino acids, of the protein was shown to be mostly mediated by hydrogen bonding.

The results of the docking simulations revealed a good binding behavior of the Co-complex to the protein in the current investigation. For Gram-positive bacteria (*Staphylococcus Aureus* 3ty7), a number of amino acids in the protein could interact with the complex functional centers resulting in a good *H*-bond interaction. Figures (7-9) show that the Co-complex can achieve a good interaction with all receptors and produce results that are comparable. The studied protein has easily been revealed for inter-hydrogen bonds according to visualization of the afforded interactions in two- and three-dimensional images. The latter graphics may strongly contribute to the demonstration of the mechanism of interaction within docking molecules. (Figures 7-9). The interaction between the studied complex and the amino acids of the protein was shown to be mostly mediated by hydrogen bonding in addition to other modes.

For human Gram-positive bacteria (*Staphylococcus Aureus)*, the interactions of protein amino acids with the ligand resulting in hydrogen bonds showing good binding affinities towards the active site with binding energy = − 4.8 kcal mol^{-1} (Figure 10) involving bonding with LYS`41, ALA`42, ASN`17, ALA`42, GLY`205. The studied complex also revealed interactions with 3t88 active sites related to the *Escherichia Coli* with − 6.9 kcal $mol^{-1}$ (Figure 11). The latter behavior GLN`189, SER`84, ASN`107, PRO`50, THR`52, and VAL`44. For the *Candida albicans*, 5k04 protein active site was applied in the simulation investigation showing good binding affinities with the ligand complex (fig 12), with – 7.2 kcal $mol^{-1}$. The hydrogen bonding in the latter was achieved by GLU`98, LYS`114, LYS`149, PHE`112 and ILE`150.

The behavior of the Cu complex towards the proteins also showed binding interaction with the active site of such proteins. Thus, for Gram-positive bacteria (*Staphylococcus Aureus* 3ty7), the amino acids in the protein interacted with the produced complex forming a number of *H*-bonding interactions. Such interaction mode was investigated to determine its possible binding affinities with binding energy = − 4.8 kcal mol^{-1}.

The phosphonate product **5b** also could be also able to interact with amino acid residues of 5KJU active site related to the human HTC-116 colon cancer cell line with - 10.5 kcal mol^{-1} (Figure 10). LYS`41, ALA`42, ASN`40, GLU`49, ASN`40 and ASN`17 are the participating residues in the process.

The possible interaction behavior of the Cu complex was also studied for 3t88 active site to account for the possible activity against Escherichia Coli as a type of Gram-positive species. The results showed the ability of the later product to achieve good binding affinities with certain amino acid moieties (fig 11), with – 6.9 kcal mol^{-1}. The latter interaction could be possible by SER`84, PHE`162, THR`155, ASP`163, and TYR`129 residues.

On the other hand, according to the observed results Cu-complex could be able to possess H-bonding interaction with 5k04 active site related to *Candida albicans via* ASN`117, LYS`114, GLU`70 and ARG`86 amino acids with − 10.8 kcal mol^{-1} binding energy.

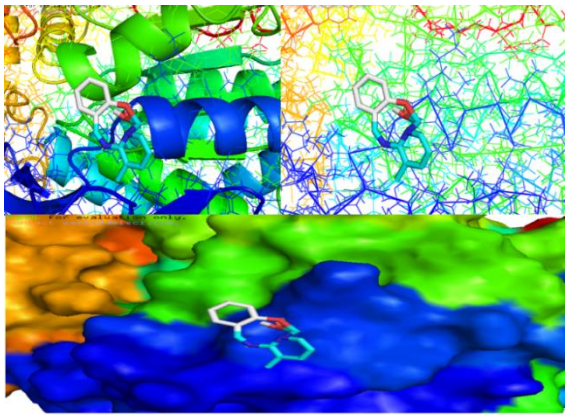

Fig. 7: Docking of Co(II) complex into 3ty7 protein.

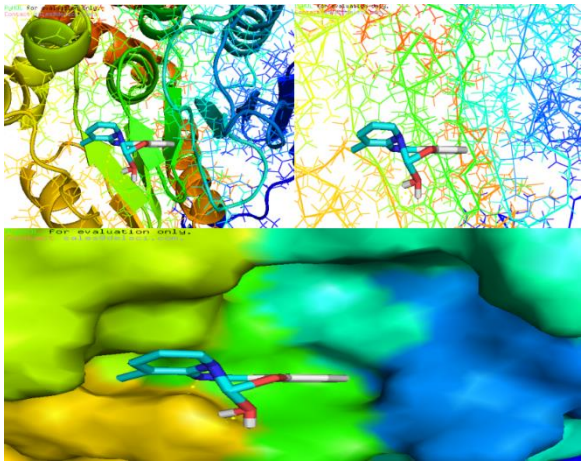

Fig. 8: Docking of Co(II) complex into 3t88 protein.

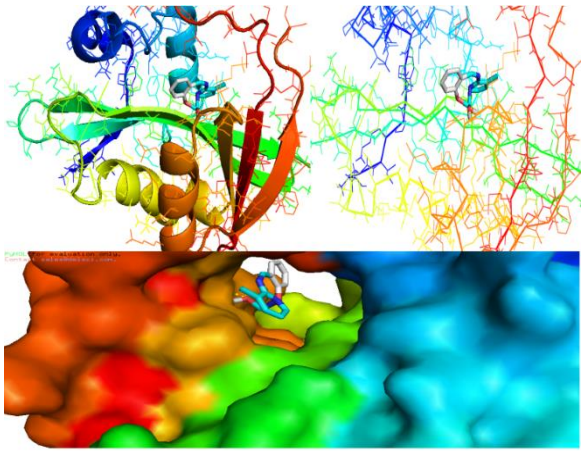

Fig. 9: Docking of Co(II) complex into 5k04 protein.

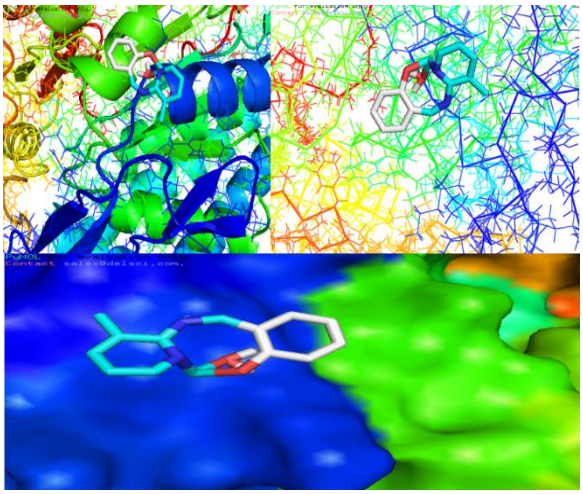

Fig. 10: Docking of Cu-complex into 3ty7 protein.

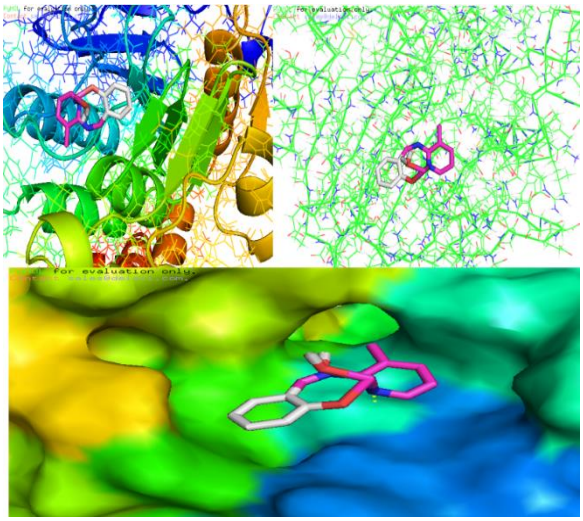

Fig. 11: Docking of Cu-complex into 3t88 protein

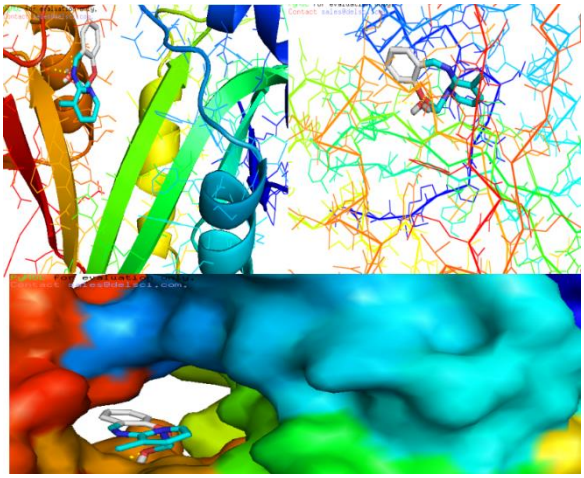

Fig. 12: Docking of Cu-complex into 5k04 protein.

4. Conclusions

A functionalized pyridyl-arylidine Shiff base legend incorporating a hydroxyl group in the ortho-position formed a number of metal complexes via coordination with (Pd(II), Co(II), Cu(II), and Ag(I)). The analytical and spectral data verified, obviously, the formulae of the Schiff base ligand and derived metal complexes. The electrolytic behaviour of the resulting metal complexes was revealed by their afforded results. Furthermore, Pd(II) as well as Cu(II) complexes exhibited square planar geometrical shapes, while Co(II) and Ag(I) complexes displayed tetrahedral geometry. Co(II) and Ag(I) formed complexes that have been shown to exist in a crystalline structure revealing a particular average size, of the crystallites. The performed thermal analysis investigation showed, that the Pd(II), Co(II) and Cu(II) complexes consistently release ligands and anionic components via the initial loss of H_2O molecules of hydration. The investigated antimicrobial activity against of a number of microorganisms demonstrated that the complexes showed much-improved activity than the free metal. Interestingly, cobalt and silver-based complexes showed potent activity against *E. coli* that were found to be more potent than those recorded for Neomycin and Ag(I) complex revealed comparable behavior. Molecular docking results demonstrated the ability of the studies product for achieving good binding interaction with the three proteins' active sites in the current investigation with good binding energies. The results open new horizons for intensifying research work on this type of compounds for developing new antibacterial agents.

Acknowledgments

The authors gratefully acknowledge Qassim University, represented by the Deanship of Scientific Research, on the financial support for this research under the number (2023-SDG-1-BSRC35386) during the academic year 1445 AH / 2023 AD.

References

[1] Prestinaci, F., Pezzotti, P., & Pantosti, A. (2015). Antimicrobial resistance: a global multifaceted phenomenon. Pathogens and global health, 109(7), 309-318.

[2] Ferraz, R., Branco, L. C., Marrucho, I. M., Araújo, J. M., Rebelo, L. P. N., da Ponte, M. N., ... & Petrovski, Ž. (2012). Development of novel ionic liquids based on ampicillin. MedChemComm, 3(4), 494-497.

[3] Amador, P., Fernandes, R., Brito, L., & Prudencio, C. (2011). Antibiotic resistance in

Enterobacteriaceae isolated from Portuguese deli meats. Journal of Food Safety, 31(1), 1-20.

[4] Amador P, Fernandes R, Duarte I, Brito L, Prudencio C. (2011). In vitro transference and molecular characterization of blaTEM genes in bacteria isolated from Portuguese ready-to-eat foods. World J Microbiol Biotechnol 27: 1775-1785.

[5] Fernandes R, Prudencio C. (2010). Post-surgical wound infections involving Enterobacteriaceae with reduced susceptibility to β-lactams in two Portuguese hospitals. Int Wound J 7: 508-514.

[6] Pennington H. (2011). Escherichia coli O104, Germany 2011. Lancet Infect Dis 11: 652-653.

[7] Bielaszewska M, Mellmann A, Zhang W, Koeck R, Fruth A, et al. (2011). Characterization of the Escherichia coli strain associated with an outbreak of haemolytic uraemic syndrome in Germany, 2011: a microbiological study. Lancet Infect Dis 11: 671-676.

[8] Tseng SH, Lee CM, Lin TY, Chang SC, Chang FY. (2011). Emergence and spread of multi-drug resistant organisms: think globally and act locally. J Microbiol Immunol Infect 44: 157-165.

[9] Kumarasamy KK, Toleman MA, Walsh TR, Bagaria J, Butt F, et al. (2010). Emergence of a new antibiotic resistance mechanism in India, Pakistan, and the UK: a molecular, biological, and epidemiological study. Lancet Infect Dis 10: 597-602.

[10] Mochon AB, Garner OB, Hindler JA, Krogstad P, Ward KW, et al. (2011). New Delhi Metallo-beta-Lactamase (NDM-1)-Producing Klebsiella pneumoniae: Case Report and Laboratory Detection Strategies. Journal of Clinical Microbiology 49: 2386.

[11] Amador P, Fernandes R, Prudencio C, Brito L. (2009). Resistance to Betalactams in Bacteria Isolated from Different Types of Portuguese Cheese. Int J Mol Sci 10: 1538-1551.

[12] Fernandes R, Vieira M, Ferraz R, Prudencio C. (2008). Bloodstream infections caused by multidrug-resistant Enterobacteriaceae: report from two Portuguese hospitals. J Hosp Infect 70: 93-95.

[13] Fernandes R, Gestoso A, Freitas JM, Santos P, Prudencio C. (2009). High resistance to fourth-generation cephalosporins among clinical isolates of Enterobacteriaceae producing extended-spectrum beta-lactamases isolated in Portugal. Int J Antimicrob Agents 33: 184-185

[14] Licata, F., Quirino, A., Pepe, D., Matera, G., & Bianco, A. (2020). Collaborative Group. Antimicrobial Resistance in Pathogens Isolated from Blood Cultures: A Two-Year Multicenter Hospital Surveillance Study in Italy. Antibiotics (Basel). 2020; 10 (1): 10.

[15] Frei, A., Zuegg, J., Elliott, A. G., Baker, M., Braese, S., Brown, C., ... & Blaskovich, M. A. (2020). Metal complexes as a promising source for new antibiotics. Chemical science, 11(10), 2627-2639.

[16] Lloyd, N. C., Morgan, H. W., Nicholson, B. K., & Ronimus, R. S. (2004). The composition of Ehrlich's salvarsan: resolution of a century-old debate.

[17] Gasser, G. (2015). Metal complexes and medicine: A successful combination. Chimia, 69(7-8), 442-442.

[18] Johnstone, T. C., Suntharalingam, K., & Lippard, S. J. (2016). The next generation of platinum drugs: targeted Pt (II) agents, nanoparticle delivery, and Pt (IV) prodrugs. Chemical reviews, 116(5), 3436-3486.

[19] Biot, C., Nosten, F., Fraisse, L., Ter-Minassian, D., Khalife, J., & Dive, D. (2011). The antimalarial ferroquine: from bench to clinic. Parasite: journal de la Société Française de Parasitologie, 18(3), 207.

[20] Monro, S., Colon, K. L., Yin, H., Roque III, J., Konda, P., Gujar, S., ... & McFarland, S. A. (2018). Transition metal complexes and photodynamic therapy from a tumor-centered approach: challenges, opportunities, and highlights from the development of TLD1433. Chemical reviews, 119(2), 797-828.

[21] Zeng, L., Gupta, P., Chen, Y., Wang, E., Ji, L., Chao, H., & Chen, Z. S. (2017). The development of anticancer ruthenium (II) complexes: from single molecule compounds to nanomaterials. Chemical Society Reviews, 46(19), 5771-5804.

[22] Kenny, R. G., & Marmion, C. J. (2019). Toward multi-targeted platinum and ruthenium drugs—a new paradigm in cancer drug treatment regimens?. Chemical reviews, 119(2), 1058-1137.

[23] https://www.clinicaltrials.gov, accessed on 5 December (2019).

[24] Korfel, A., Scheulen, M. E., Schmoll, H. J., Gründel, O., Harstrick, A., Knoche, M., ... & Berdel, W. E. (1998). Phase I clinical and pharmacokinetic study of titanocene dichloride in adults with advanced solid tumors. Clinical cancer research: an official journal of the American Association for Cancer Research, 4(11), 2701-2708.

[25]https://www.ema.europa.eu/en/medicines/human/EPAR/ tookad, accessed 09.10.(2019).

[26] Gasser, G., & Metzler-Nolte, N. (2012). The potential of organometallic complexes in medicinal chemistry. Current opinion in chemical biology, 16(1-2), 84-91.

[27] Gianferrara, T., Bratsos, I., & Alessio, E. (2009). A categorization of metal anticancer

compounds based on their mode of action. Dalton Transactions, (37), 7588-7598.
[28] Morrison, C. N., Prosser, K. E., Stokes, R. W., Cordes, A., Metzler-Nolte, N., & Cohen, S. M. (2020). Expanding medicinal chemistry into 3D space: Metallofragments as 3D scaffolds for fragment-based drug discovery. Chemical science, 11(5), 1216-1225.
[29] Al-Fakeh, M. S., Alsikhan, M. A., & Alnawmasi, J. S. (2023). Physico-Chemical Study of Mn (II), Co (II), Cu (II), Cr (III), and Pd (II) Complexes with Schiff-Base and Aminopyrimidyl Derivatives and Anti-Cancer, Antioxidant, Antimicrobial Applications. Molecules, 28(6), 2555.
[30] El-Ghoul, Y., Al-Fakeh, M. S., & Al-Subaie, N. S. (2023). Synthesis and Characterization of a New Alginate/Carrageenan crosslinked biopolymer and Study of the Antibacterial, Antioxidant, and Anticancer Performance of its Mn (II), Fe (III), Ni (II), and Cu (II) polymeric complexes. Polymers, 15(11), 2511.
[31] N. K. Chaudhary, B. Guragain, S. K. Chaudhary, and P. Mishra, "Schiff base metal complex as a potential therapeutic drug in medical science: A critical review," Bibechana, vol. 18, no. 1, pp. 214–230, 2021, doi: 10.3126/bibechana.v18i1.29841.
[32] Johnson, P., George, G., Ramalingam, S., & Periandy, S. (2018). Spectroscopic and QSAR analysis on Antibiotic drug; 2-amino-4, 6-dimethylpyrimidine using Quantum Computational Tools. J Mol Pharm Org Process Res, 6(142), 2.
[33] Al-Fakeh, M. S., & Al-Otaibi, N. F. (2022). Nd_2O_3, Cr_2O_3, and V_2O_3 Nanoparticles via calcination: synthesis, characterization, antimicrobial and antioxidant activities. Journal of Nanotechnology, 2022.
[34] Al-Fakeh, M. S., Allazzam, G. A., & Yarkandi, N. (2021). Preparation, Properties and Antimicrobial evaluation of a new metal complex with Diphosphine ligand and 2-Aminopyridine, SYLWAN., 165(9), 9.
[35] Al-Fakeh, M. S., Allazzam, G. A., & Yarkandi, N. H. (2021). Ni (II), Cu (II), Mn (II), and Fe (II) Metal Complexes Containing 1, 3-Bis (diphenylphosphino) propane and Pyridine Derivative: Synthesis, Characterization, and Antimicrobial Activity. International Journal of Biomaterials, 2021.
[36] Singh, P. (Ed.). (2022). Recent developments in the synthesis and applications of pyridines.
[37] Al-Fakeh, M. S., Alsikhan, M. A., Alnawmasi, J. S., & Al-Wahibi, M. S. (2024). New Nanosized V (III), Fe (III), and Ni (II) Complexes Comprising Schiff Base and 2-Amino-4-Methyl Pyrimidine: Synthesis, Properties, and Biological Activity. International Journal of Biomaterials, 2024(1), 9198129.
[38] El-Sayed, W. A., Metwally, M. A., Nada, D. S., Mohamed, A. A., & Abdel-Rahman, A. A. H. (2013). Synthesis and Antimicrobial Activity of New Substituted 5-(Pyridine-3-yl)-1, 3, 4-Thiadiazoles and Their Sugar Derivatives. Journal of Heterocyclic Chemistry, 50(2), 194-201.
[39] Kassem, A. F., Omar, M. A., Nossier, E. S., Awad, H. M., & El-Sayed, W. A. (2023). Novel pyridine-thiazolidinone-triazole hybrid glycosides targeting EGFR and CDK-2: Design, synthesis, anticancer evaluation, and molecular docking simulation. Journal of Molecular Structure, 1294, 136358.
[40] Samiee, S., Shiralinia, A., Hoveizi, E., & Gable, R. W. (2022). A new Pd (II) complex containing acetophenone oxime and 1, 3-Bis (diphenylphosphino) propane ligands; crystal structure, catalytic activity, molecular docking and in vitro cytotoxic evaluation. Inorganica Chimica Acta, 538, 120964.
[41] A. K. Hijazi, Z. A. Taha, N. J. Abuhamad, W. M. Al-Momani. (2021). Journal of Saudi Chemical Society, 25, 10187.
[42] Zayed, E. M., El-Sayed, W. A., Abd El Salam, H. A., & Mohamed, G. G. (2023). Computer modeling, docking, spectroscopic analysis, and antibacterial testing of metal chelates with dioxatetraaza ligand. Egyptian Journal of Chemistry, 66(13), 1915-1925.
[43] Hawata, M. A., El-Essawy, F., El-Sayed, W. A., & El-Bayaa, M. (2022). Synthesis and Cytotoxic Activity of New Substituted Pyrazolo [3, 4-b] pyridine Derivatives and Their Acyclic Nucleoside Analogs. Egyptian Journal of Chemistry, 65(3), 161-169.
[44] Jiang, Y., Zhang, W., Han, M., Wang, X., Solan, G. A., Wang, R., ... & Sun, W. H. (2022). Phenoxy-imine/-amide aluminum complexes with pendant or coordinated pyridine moieties: Solvent effects on structural type and catalytic capability for the ROP of cyclic esters. Polymer, 242, 124602.
[45] Zayed, E. M., Ewies, E. F., Hassaballah, A. I., & Mohamed, G. G. (2023). Synthesis, characterization, DFT, docking, antimicrobial and thermal study of pyrimidine-carbonitrile ligand and its metal complexes. Journal of Molecular Structure, 1284, 135396.
[46] El Malah, T., Nour, H. F., Satti, A. A., Hemdan, B. A., & El-Sayed, W. A. (2020). Design, synthesis, and antimicrobial activities of 1, 2, 3-triazole glycoside clickamers. Molecules, 25(4), 790.

[47] Sarker, S. D., Nahar, L., & Kumarasamy, Y. (2007). Microtitre plate-based antibacterial assay incorporating resazurin as an indicator of cell growth, and its application in the in vitro antibacterial screening of phytochemicals. Methods, 42(4), 321-324.

[48] Chohan, Z. H., Munawar, A., & Supuran, C. T. (2001). Transition metal ion complexes of Schiff-bases. Synthesis, characterization and antibacterial properties. Metal-based drugs, 8, 137-143.

[49] Al-Fakeh, M. S., & Alsaedi, R. O. (2021). Synthesis, characterization, and antimicrobial activity of CoO nanoparticles from a Co (II) complex derived from polyvinyl alcohol and aminobenzoic acid derivative. The Scientific World Journal, 2021.

[50] Al-Fakeh, M. S. (2017). Facile Preparation of a Nanostructured Silver Oxide from a Mixed Ligand Coordination Polymer: Characterization and Biological Activity. Adv. Res., 1-8.

[51] Al-Fakeh, M. S. (2018). Synthesis and characterization of coordination polymers of 1, 3-di (4-pyridyl)-propane and 2-aminobenzothiazole with Mn (II), Co (II), Cu (II) and Ni (II) ions. Journal of Chemical and Pharmaceutical Research, 10(2), 77-83.

[52] Wellington, K. W., Kaye, P. T., & Watkins, G. M. (2009). Designer ligands. Part 14. Novel Mn (lI), Ni (II) and Zn (II) complexes of benzamide-and biphenyl-derived ligands.

[53] Jin, Q. H., Hu, K. Y., Song, L. L., Wang, R., Zhang, C. L., Zuo, X., & Lu, X. M. (2010). Synthesis and structural characterisation of five copper (I) and silver (I) complexes with 2-aminopyridine (2-APy),[Cu (μ-Cl)(2-Apy)(PPh3)] 2,[Ag (μ-X)(2-Apy)(PPh3)] 2 (X= Cl, Br),[Ag (μ-ONO2)(2-Apy)(EPh3)] 2 (E= P, As). Polyhedron, 29(1), 441-445.

[54] El-Boraey, H. A., & El-Din, A. A. S. (2014). Transition metal complexes of a new 15-membered [N5] penta-azamacrocyclic ligand with their spectral and anticancer studies. Spectrochimica Acta Part A: Molecular and Biomolecular Spectroscopy, 132, 663-671.

[55] Aly, S. A. (2018). Physico-chemical study of new ruthenium (III), Pd (II) and Co (II) complexes, DNA binding of Pd (II) complex and biological applications. Journal of Radiation Research and Applied Sciences, 11(3), 163-170.

[56] Joseyphus, R. S., & Nair, M. S. (2010). Synthesis, characterization and biological studies of some Co (II), Ni (II) and Cu (II) complexes derived from indole-3-carboxaldehyde and glycylglycine as Schiff base ligand. Arabian Journal of Chemistry, 3(4), 195-204.

[57] Masoud, M. S., Hagagg, S. S., Ali, A. E., & Nasr, N. M. (2012). Synthesis and spectroscopic characterization of gallic acid and some of its azo complexes. Journal of Molecular Structure, 1014, 17-25.

[58] Deivanayagam, P., Bhoopathy, R. P., & Thanikaikarasan, S. (2014). Synthesis, characterization, antimicrobial, analgesic and CNS studies of Schiff base Cu (II) complex derived from 4-choro-o-phenylene Diamine. Int. J. Adv. Chem, 2(2), 166-170.